SIMULATIONS OF A MAGNETIC PULSE COMPRESSOR

C. D. Boley
Lawrence Livermore National Laboratory, Livermore, CA 94550 USA

Abstract

The 3-stage magnetic pulse compressor MAG 1-D has been modeled with a code which calculates the hysteresis behavior of magnetic cores placed within a circuit. The voltage waveforms are shown to compare favorably with data taken by Barrett. A speculative modification to MAG 1-D, suggested by the reset behavior of the model, is discussed.

Introduction

This paper is devoted to numerical simulations of the magnetic pulse compressor MAG 1-D, which is used in the linear electron accelerator ETA-II. A circuit diagram of MAG 1-D is shown in Fig. 1, and the parameter values are listed in Table 1. Very schematically, the device operates as follows. The energy storage capacitor C_0 is initially charged to 25.5 kV. After the thyratron fires, the energy is transferred to the precompression capacitor C_1, with a charge time of about 3.8 μs. The magnetic switch L_1 then saturates, allowing the energy to flow through the 1:10 transformer and to charge the capacitor C_2 (charge time about 1 μs). After the switch L_2 saturates, the energy is transferred to a coaxial cable pulse-forming line (electrical length 35 ns), which has a charge time of about 200 ns. At this point, the third magnetic switch saturates and the energy is applied to the load, which is here treated as a simple resistor. The unabsorbed energy then reflects back through the circuit. The cores in MAG 1-D are reset by two circuits, as shown in Fig. 1. All cores are wound with Metglas 2605CO.

We model this device making use of a core model discussed earlier [1]. Magnetic hysteresis is treated by a rate-dependent theory developed recently by Hodgdon [2]. Rate dependence is found to play an important role in the second stage and a crucial role in the third stage.

The voltage waveforms are compared with data taken by Barrett [3]. At the beginning, there is essentially complete agreement, while at the end, the main pulse is accurate to within about 20%. Only a single cycle of duration 200 μs was simulated.

The first reset current is found to undergo wide swings with a period of about 70 μs and an amplitude of about 100 amps. Consequently, the first stage switch does not reset properly, and the precompression capacitor (input to the first stage) undergoes multiple voltage oscillations. To investigate whether this reset behavior could be corrected, the model was modified so as to contain a single isolated reset rod. The reset current then settled down, and the precompression capacitor showed only a single late-time oscillation. The behavior of the pulse itself (for one cycle) was practically unaffected.

Model

In the core model [1] employed here, the magnetic field within the cores, in both the switches and the transformer, is taken to be azimuthal and to depend only on time, and the displacement current is assumed negligible. Thus the voltage across the core can be shown to satisfy $V(t) = L(t)\, dI(t)/dt$, where the time-dependent inductance is

$$L(t) = \frac{N_w^2 h}{2\pi} \int_{r_{in}}^{r_{out}} \frac{\mu(r,t)}{r}\, dr \approx \frac{N^2 h}{2\pi} \ln\left(\frac{r_{out}}{r_{in}}\right) \mu(t). \qquad (1)$$

Here μ is the time-dependent permeability, h is the height of a core, N_w is the number of windings, and r_{in} and r_{out} are the inner radius and outer radius, respectively. We have ignored the radial dependence of the fields, which typically is an effect of order 10%. The magnetic field itself evolves according to the derivative of Ampere's law, or $\dot{B} = \mu NV/(2\pi \bar{r} L)$, with $\bar{r} = (r_{out} - r_{in})/\ln(r_{out}/r_{in})$.

The complications of hysteresis reside in μ, which, in the Hodgdon theory, depends on B, $\dot{B}$, and H according to an equation of the form

$$\mu(B, H, \dot{B}) = \{\alpha\, \mathrm{sign}(\dot{B})\, [f(B) - H] + g(B, \dot{B})\}^{-1}, \qquad (2)$$

where α is a constant and f and g are functions particular to the magnetic material. The fact that the permeability depends on the sign of $\dot{B}$ leads to hysteresis. This theory reproduces many of the known features of hysteresis phenonmena, such as loop closure near saturation, the formation of minor loops, and loop broadening with increasing $\dot{B}$. The functions appropriate to Metglas 2605CO are given in the Appendix. In a previous application [1], this combination of core model and hysteresis model was shown to give quite satisfactory agreement with experiment.

We employ a simple thyratron model, which, for positive currents, is a negative 500 v source. This accounts for the forward drop across the thyratron. For negative currents, the thyratron is modeled as a 1000 ohm resistor in series with the same source.

The coaxial cable PFL is treated as a series of N stages, each containing a parallel capacitor C/N and resistor NG, with a series inductor $L/2N$ and resistor $R/2N$ on each side (cf. Table 1). Here R accounts for the total ESR of the line, and G accounts for the conductivity of water. The simulations reported here have $N = 10$ stages.

The equations of the model are set up as a system of ODEs. In the problem at hand, the system has 54 variables, including magnetic fields within the cores. Owing to the presence of rate-dependent hysteresis, the equations have extreme nonlinearities. The system is

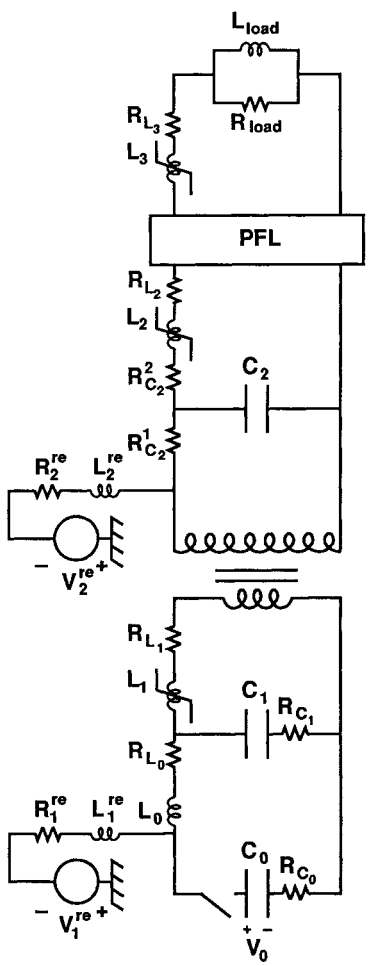

Fig. 1. MAG 1-D circuit.

Report Documentation Page

Form Approved
OMB No. 0704-0188

Public reporting burden for the collection of information is estimated to average 1 hour per response, including the time for reviewing instructions, searching existing data sources, gathering and maintaining the data needed, and completing and reviewing the collection of information. Send comments regarding this burden estimate or any other aspect of this collection of information, including suggestions for reducing this burden, to Washington Headquarters Services, Directorate for Information Operations and Reports, 1215 Jefferson Davis Highway, Suite 1204, Arlington VA 22202-4302. Respondents should be aware that notwithstanding any other provision of law, no person shall be subject to a penalty for failing to comply with a collection of information if it does not display a currently valid OMB control number.

1. REPORT DATE	2. REPORT TYPE	3. DATES COVERED
JUN 1991	**N/A**	**-**

4. TITLE AND SUBTITLE
Simulations Of A Magnetic Pulse Compressor

5a. CONTRACT NUMBER
5b. GRANT NUMBER
5c. PROGRAM ELEMENT NUMBER

6. AUTHOR(S)

5d. PROJECT NUMBER
5e. TASK NUMBER
5f. WORK UNIT NUMBER

7. PERFORMING ORGANIZATION NAME(S) AND ADDRESS(ES)
Lawrence Livermore National Laboratory, Livermore, CA 94550 USA

8. PERFORMING ORGANIZATION REPORT NUMBER

9. SPONSORING/MONITORING AGENCY NAME(S) AND ADDRESS(ES)

10. SPONSOR/MONITOR'S ACRONYM(S)
11. SPONSOR/MONITOR'S REPORT NUMBER(S)

12. DISTRIBUTION/AVAILABILITY STATEMENT
Approved for public release, distribution unlimited

13. SUPPLEMENTARY NOTES
See also ADM002371. 2013 IEEE Pulsed Power Conference, Digest of Technical Papers 1976-2013, and Abstracts of the 2013 IEEE International Conference on Plasma Science. Held in San Francisco, CA on 16-21 June 2013. U.S. Government or Federal Purpose Rights License

14. ABSTRACT
The 3-stage magnetic pulse compressor MAG 1-D has been modeled with a code which calculates the hysteresis behavior of magnetic cores placed within a circuit. The voltage waveforms are shown to compare favorably with data taken by Barrett. A speculative modification to MAG 1-D, suggested by the reset behavior of the model, is discussed.

15. SUBJECT TERMS
4

16. SECURITY CLASSIFICATION OF:			17. LIMITATION OF ABSTRACT	18. NUMBER OF PAGES	19a. NAME OF RESPONSIBLE PERSON
a. REPORT	b. ABSTRACT	c. THIS PAGE			
unclassified	**unclassified**	**unclassified**	**SAR**	**4**	

advanced in time by the solver LSODAR, which is a variant of the standard package LSODE [4].

Results

We now turn to a full 200 μs simulation of the device. At $t = 0$, the intermediate energy storage capacitor C_0 is charged to 25.5 kV, and the reset currents are assigned their static values. Figure 2 shows the calculated voltage across C_1, along with data taken by Barrett. The main pulse is very close to the data, but the reflected pulse is about 20% smaller than experiment. In Fig. 3 this voltage is shown on a long time scale. The most conspicuous feature here is the sudden reversals at 35, 100, and 175 μs, which are caused by resaturations of the magnetic switch in this stage. Similar reversals are seen experimentally.

Figure 4 shows the B-H loop of the first magnetic switch. Note that the curve balloons to the right, tucks in somewhat, and then saturates. After the second saturation, however, the fields wander around and fail to reset properly. The reason for this can be seen in Fig. 5, which shows the reset currents as functions of time. The first reset current oscillates greatly and reaches negative maxima in synchronization with the current through the magnetic switch. This problem seems not to be present in the second reset current. It reaches a maximum about when the third magnetic switch saturates, and then quickly settles down.

Figure 6 shows the voltage across the water capacitor C_2, along with the experimental trace. It has a charge time of 1.2 μs, a peak of

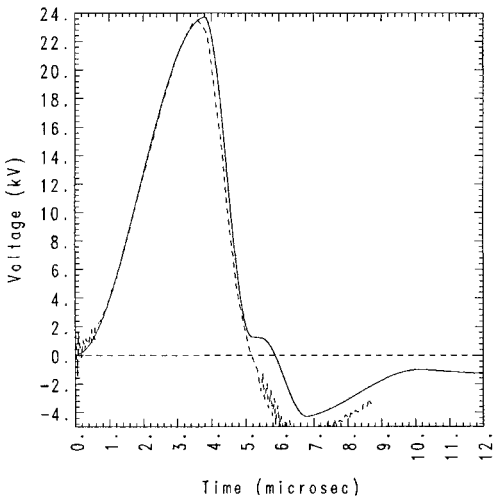

Fig. 2. Voltage across C_1 (short time scale). The dotted line indicates Barrett's data [Ref. 3].

Table 1. MAG 1-D parameter values

	Stage 1	Stage 2	Stage 3
Number of cores	3	4	3
Number of windings	2	3	1
Inner radius (cm)	8.89	8.73	11.43
Outer radius (cm)	15.24	18.73	18.73
Core height (cm)	5.08	5.08	5.08
Saturated inductance (nH)	141	631	27.3
Stray inductance (nH)	50	240	5
R_L (mΩ)	.375	6.19	.77
Packing factor	.67	.67	.55

Transformer parameters:
Number of turns: 10
Number of series cores: 4
Core height: 5.08 cm
Inner radius: 8.89 cm
Outer radius: 16.35 cm
Saturated inductance: 52.9 nH
Packing factor: .67
Primary ESR: .3 mΩ
Secondary ESR: 89 mΩ

PFL parameters:
Inner radius: 16.19 cm
Outer radius: 22.23 cm
Length: 116.8 cm
$C = 17.3$ nF
$L = 74$ nH
$R = .07\ \Omega$
$G = 7770\ \Omega$

$L_0 = 1.5\ \mu$H	$R_{L_0} = 4.35$ mΩ	$V_1^{re} = 20$ v
$C_0 = 2\ \mu$F	$R_{C_0} = 21$ mΩ	$R_1^{re} = 1\Omega$
$C_1 = 2.1\ \mu$F	$R_{C_1} = 7$ mΩ	$L_1^{re} = 150\mu$H
$C_2 = 19.3$ nF	$R_{C_2}^1 = 740$ mΩ	$V_2^{re} = 50$ v
$R_{\text{load}} = 2.1\ \Omega$	$R_{C_2}^2 = 46$ mΩ	$R_2^{re} = 2.5\ \Omega$
$L_{\text{load}} = 10\ \mu$H		$L_2^{re} = 4.35$ mH

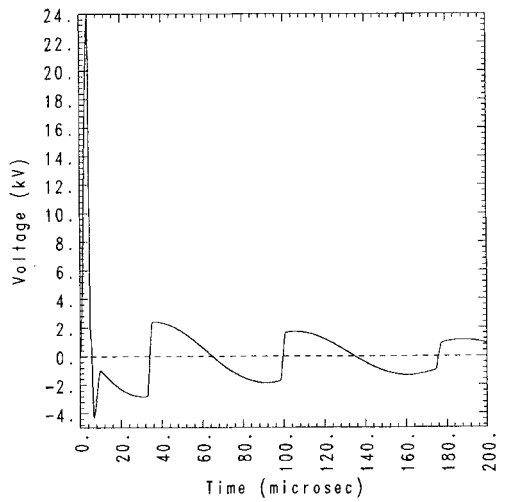

Fig. 3. Voltage across C_1 (long time scale).

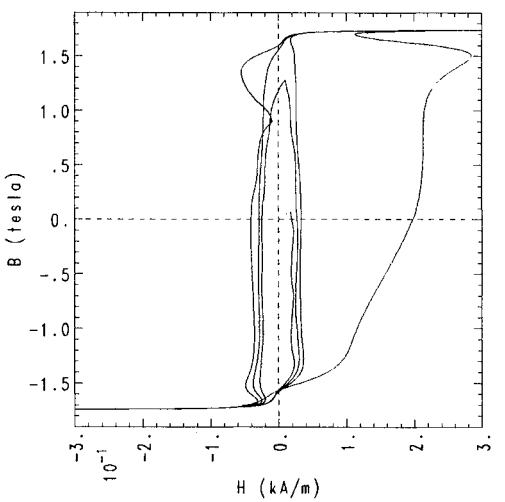

Fig. 4. B-H loop of magnetic switch in stage 1.

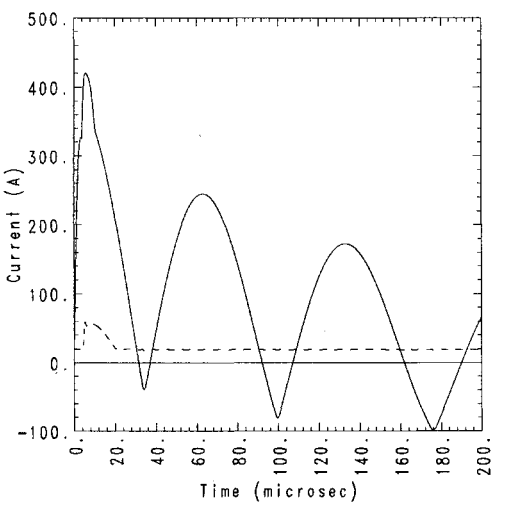

Fig. 5. First reset current (full line) and second reset current (dashed line).

230 kV, and a discharge time of about 200 ns, all in reasonable agreement with Barrett's measurements. The B-H loop of the magnetic switch in this stage is shown in Fig. 7. Before the first saturation, it balloons about twice as far to the right as the previous switch, as it experiences more severe rate dependence. Afterwards, it resaturates and then appears to reset normally.

The voltage across the output of the PFL is shown in Fig. 8. Its maximum (210 kV) is about 10% higher than experiment. Note that it falls in about 10 ns to half maximum, momentarily reverses, and then falls in another 10 ns to zero. This behavior can probably be traced to the interplay of forward and backward waves. A similar pattern is observed in experiment. The multiple reflections following the pulse have a period of twice the electrical length of the PFL, or 70 ns. These also show up on the experimental trace.

Figure 9 shows the B-H loop of the magnetic switch in the third stage. It is wider by a factor of four than that in the previous switch. The multiple reflections in the PFL show up here in a picturesque way, and the switch appears to reset properly.

Figure 10 shows the calculated and observed voltages across the load. The calculated peak of 118 kV is about 20% higher than experiment, but the widths (about 60 ns) agree well.

Turning to the final energy balance, we find that the load dissipates 467 joules. The greatest unwanted energy loss occurs in the thyratron, which dissipates 34 joules. Hysteresis losses in the third stage account for the next most serious loss (29 joules).

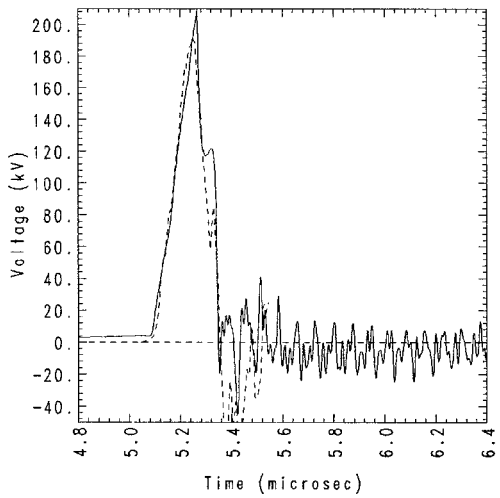

Fig. 8. Voltage across output of PFL. The dotted line indicates Barrett's data.

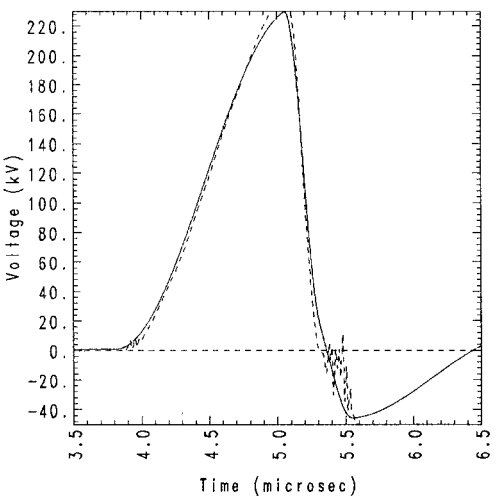

Fig. 6. Voltage across C_2. The dotted line indicates Barrett's data.

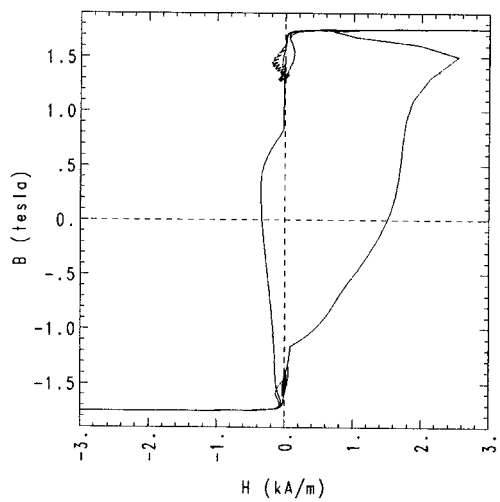

Fig. 9. B-H loop of magnetic switch in stage 3.

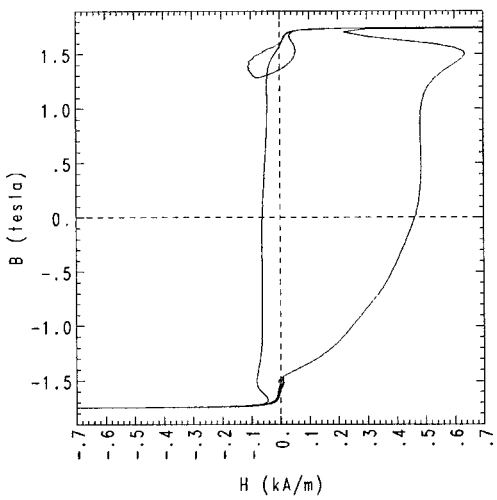

Fig. 7. B-H loop of magnetic switch in stage 2.

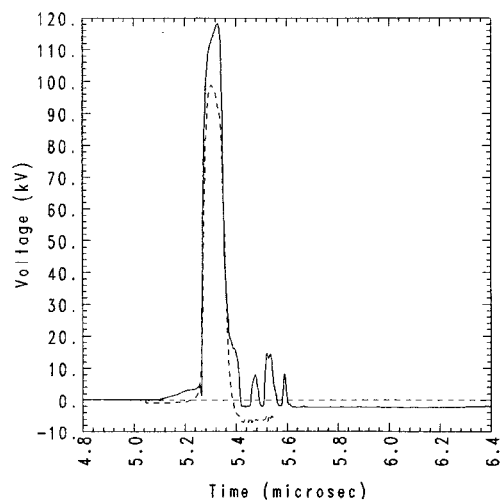

Fig. 10. Voltage across load. The dotted line indicates Barrett's data.

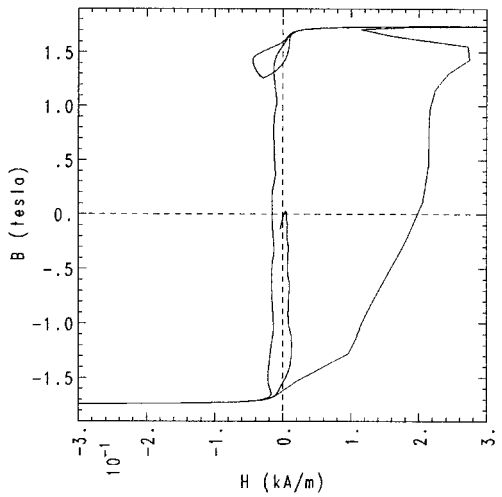

Fig. 11. B-H loop of switch in stage 1 (alternate case).

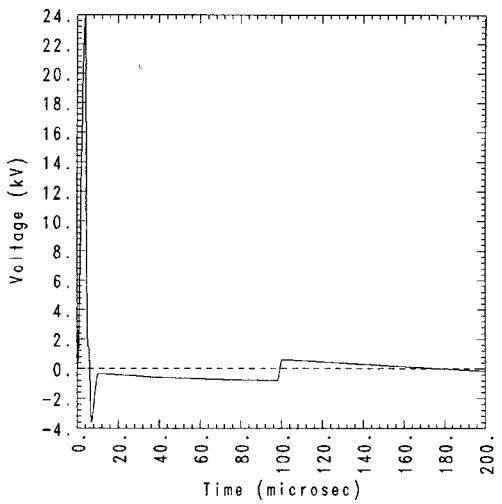

Fig. 12. Voltage across C_1 (alternate case).

Alternate Case

To see whether the reset problem observed in the previous run could be improved, at least conceptually, the modulator was imagined to be reconfigured such that an isolated reset rod passed axially through the centers of all the cores. (This is possible only if all stages are configured with their fluxes pointing in the same direction.) In the simulation the reset rod was connected to a voltage source of 20 v, with a 1 ohm resistor and a large inductor (10 mH) in series. All other run conditions remained the same as above.

The resulting reset current is stable and well-behaved, rising by 50% and then settling back toward its equilibrium value of 20 amps. Hence the first switch also settles down, as shown by its B-H loop in Fig. 11. Note that the cores have not quite fully resaturated even after 200 μs; some further refinement of the reset parameters might be necessary to achieve a complete reset. The voltage across C_1 now undergoes only a single late-time oscillation, at about 100 μs, as seen in Fig. 12. This figure should be compared with Fig. 3, showing the multiple oscillations observed with the original reset scheme. The other switches and the PFL perform much as in the previous case. The voltage across the load has virtually the same shape as in the previous case.

Conclusions

These simulations show that the MAG 1-D modulator can be modeled with quite reasonable accuracy. Hence the code could serve as a useful guide in trouble-shooting and in the design of possible modifications to the device.

As a specific example of such interplay between model and experiment, the results indicate that the first stage does not reset properly in the base case. An alternative reset mechanism was set up and shown to give better performance.

Acknowledgments

The author would like to thank E. G. Cook for providing him with the MAG 1-D parameter values, and W. A. Molander, D. G. Ball, D. M. Barrett, A. C. Hindmarsh, and B. E. Warner for discussions. He is also grateful to G. D. Duckworth for computational assistance.

This work was performed under the auspices of the U.S. Department of Energy by Lawrence Livermore National Laboratory under contract No. W-7405-Eng-48.

Appendix

In the version of the Hodgdon theory used here, the material functions f and g have the form

$$f(B) = \begin{cases} A_1(\tan(A_2 B))^p + f_{ex}B, & 0 \le B \le B_{bp}; \\ A_1(\tan(A_2 B_{bp}))^p + f_{ex}B_{bp} + (B - B_{bp})/\mu_s, & B > B_{bp}; \\ -f(-B), & B < 0; \end{cases} \tag{A1}$$

$$g(B,\dot{B}) = \begin{cases} f'(B)\Big[1 - A_3\ c(\dot{B}) \exp(-\dfrac{A_4|B|}{B_{cl} - |B|})\Big], & \text{if } |B| < B_{cl}; \\ f'(B), & \text{otherwise.} \end{cases} \tag{A2}$$

The function $c(\dot{B})$, which controls the rate dependence, is given by

$$c(\dot{B}) = \begin{cases} 1 + c_1|\dot{B}|, & |\dot{B}| < \dot{B}_1; \\ 1 + c_1\dot{B}_1 + c_2(|\dot{B}| - \dot{B}_1), & \dot{B}_1 \le |\dot{B}| \le \dot{B}_2; \\ 1 + c_1\dot{B}_1 + c_2(\dot{B}_2 - \dot{B}_1) + c_3(|\dot{B}| - \dot{B}_2), & |\dot{B}| \ge \dot{B}_2. \end{cases} \tag{A3}$$

For Metglas 2605CO, the values of the constants are, in mks units:

$B_{cl} = 1.7$	$A_1 = .05809$	$c_1 = 1.1 \text{ x } 10^{-4}$	$\dot{B}_1 = 1 \text{ x } 10^5$
$B_{bp} = 1.75$	$A_2 = .8941$	$c_2 = 6.17 \text{ x } 10^{-5}$	$\dot{B}_2 = 3 \text{ x } 10^6$
$f_{ex} = .7958$	$A_3 = -26.23$	$c_3 = 3.061 \text{ x } 10^{-5}$	$\dot{B}_3 = 2.1 \text{ x } 10^7$
$p = 2$	$A_4 = .3101$	$\mu_s = .582\mu_0$	$\alpha = 10$

References

[1] C. D. Boley and M. L. Hodgdon, "Model and Simulations of Hysteresis in Magnetic Cores," IEEE Trans. Magnetics **25**, 3922 (1989).

[2] M. L. Hodgdon, "Applications of a Theory of Ferromagnetic Hysteresis," IEEE Trans. MAG-24, 218 (1988); M. L. Hodgdon, "Mathematical Theory and Calculations of Magnetic Hystersis Curves," 4th Joint MMM-Intermag Conference, Vancouver, B.C., 1988.

[3] D. M. Barrett, "MAG 1D Energy Flow Measurements and Analysis," Lawrence Livermore National Laboratory (unpublished).

[4] A. C. Hindmarsh, "ODEPACK, a Systematized Collection of ODE Solvers," in Scientific Computing, R. S. Stepleman et al. (eds.), North-Holland, Amsterdam, 1983 (Vol. I of IMACS Transactions on Scientific Computing), pp. 55–64.